

## RESEARCH ARTICLE

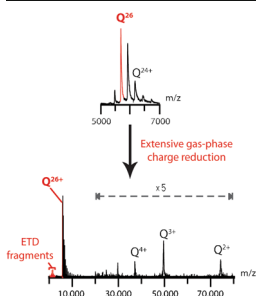
# Extensive Charge Reduction and Dissociation of Intact Protein Complexes Following Electron Transfer on a Quadrupole-Ion Mobility-Time-of-Flight MS

Frederik Lermyte,<sup>1,2</sup> Jonathan P. Williams,<sup>3</sup> Jeffery M. Brown,<sup>3</sup> Esther M. Martin,<sup>1</sup> Frank Sobott<sup>1,2</sup>

<sup>1</sup>Biomolecular and Analytical Mass Spectrometry group, Department of Chemistry, University of Antwerp, Groenenborgerlaan 171, 2020, Antwerp, Belgium

<sup>2</sup>Center for Proteomics (CFP-CeProMa), University of Antwerp, Antwerp, Belgium

<sup>3</sup>Waters Corporation, Stamford Avenue, Altrincham Road, Wilmslow, SK9 4AX, UK



**Abstract.** Non-dissociative charge reduction, typically considered to be an unwanted side reaction in electron transfer dissociation (ETD) experiments, can be enhanced significantly in order to reduce the charge state of intact protein complexes to as low as 1+ on a commercially available Q-IM-TOF instrument. This allows for the detection of large complexes beyond 100,000  $m/z$ , while at the same time generating top-down ETD fragments, which provide sequence information from surface-exposed parts of the folded structure. Optimization of the supplemental activation has proven to be crucial in these experiments and the charge-reduced species are most likely the product of both proton transfer (PTR) and non-dissociative electron transfer (ETnD) reactions that occur prior to the ion mobility cell. Applications of this approach range

from deconvolution of complex spectra to the manipulation of charge states of gas-phase ions.

**Keywords:** Top-down fragmentation, Electron transfer dissociation, Noncovalent complex, Charge state reduction, Protein complex

Received: 26 September 2014/Revised: 25 February 2015/Accepted: 1 March 2015/Published Online: 11 April 2015

## Introduction

Mass spectrometry (MS) has the ability to provide both molecular mass and sequence information of biomolecules, following their ionization [1, 2]. In electrospray ionization (ESI), proteins typically exhibit multiple charges that result from protonation of solvent accessible sites. The number of charges ( $z$ ) can be high, either because the proteins are unfolded, or as a consequence of their large mass and size. The charge state distribution of an ion is an important indicator of its three-dimensional structure in the gas phase, and for proteins it is generally believed to be closely linked to their folding state [3].

Under non-denaturing conditions (“native MS”), nano-electrospray ionization is commonly used. DC and rf-voltages

together with instrumental gas pressures are tuned such that weak biomolecular interactions are preserved and maintained during analysis. Native MS involves the ionization, transmission, and detection of intact, noncovalently assembled protein–protein, protein–DNA/RNA, and protein–ligand complexes [2, 4, 5]. Spectra typically contain relatively narrow charge state distributions at comparatively high  $m/z$ . However, because of the presence of potentially overlapping charge states and significant peak widths, charge state assignment can still be challenging, particularly for polydisperse samples or in complex mixtures. As a result, a number of specialized algorithms have been proposed to deconvolute these spectra and identify the components [6–12]. Another approach is to minimize mass spectral complexity by reducing the charge state of the ions in the gas phase by means of “charge-stripping” [13–17]. In these experiments, charge reduction and the subsequent transmission and detection of the resulting extremely high  $m/z$  species typically require instrument modifications [15, 18]. Limited charge reduction is also typically observed as a side reaction in electron capture (ECD) and electron transfer dissociation (ETD) experiments, without instrument modification,

**Electronic supplementary material** The online version of this article (doi:10.1007/s13361-015-1124-z) contains supplementary material, which is available to authorized users.

Correspondence to: Frank Sobott; e-mail: frank.sobott@uantwerpen.be

particularly when working with intact proteins [19–24]. In addition, ECD or ETD fragments can remain bound to each other by noncovalent interactions so that they appear as charge-reduced precursor ions in the spectra [24–27]. In some cases, this limited charge reduction can be sufficient to resolve complex spectra where mass and charge state assignment are otherwise not trivial [28]. Here we describe a new approach to manipulate the ion charge state using unmodified, ETD-enabled QTOF type instruments (Synapt G2 and G2-S, Waters Corporation, Wilmslow, UK) with standard ETD reagents [29–32], and propose the term “charge-reduction ETD” or short “crETD” for it, in analogy to “charge reduction electrospray mass spectrometry” (CREMS) introduced by Smith and colleagues [13, 14]. Using this methodology, we are able to observe ions with a reduced net positive charge as low as 1+ from native protein complexes, whilst also generating product ions that yield sequence-specific information within the same experiment. Importantly, the ability to manipulate charge states in the gas phase over such a wide range also opens up new possibilities for the investigation of electrostatic effects on the folding state of protein ions in the gas phase, independent of how they were generated, and to minimize the effect of charge repulsion on native structures [33, 34]. An interesting study in this regard was recently carried out by Campuzano and Schnier, who used a corona discharge to induce significant charge reduction of peptides and proteins on a Synapt HDMS instrument [35, 36]. However, as with earlier charge reduction studies mentioned above, this required instrument modification. Also, the observed charge reduction was limited, as no detection of signals above approximately 18,000  $m/z$  was reported. Furthermore, as charge reduction occurred in the source region of the instrument, a specific precursor could not be selected by using the quadrupole mass filter of the instrument in this case, an issue that is addressed by the approach described here.

## Experimental

Five proteins, all of which self-assemble into larger oligomers in their native state, were chosen to demonstrate extensive charge reduction by ETD: hemoglobin (*Bos taurus*, Sigma H2500, 64 kDa), concanavalin a (*Canavalia ensiformis*, Sigma C2010, 103 kDa), alcohol dehydrogenase (*Saccharomyces cerevisiae*, Sigma A3263, 148 kDa), pyruvate kinase (*Oryctolagus cuniculus*, Sigma P9136, 233 kDa), and L-glutamic dehydrogenase (*Bos taurus*, Sigma G7882, 336 kDa). L-glutamic dehydrogenase is hexameric, whereas the other four proteins form tetramers. The lyophilized proteins were dissolved at a concentration of 1 mg/mL in 100 mM aqueous ammonium acetate (pH=6.8) and desalted twice using Bio-Rad Micro Bio-Spin 6 columns, yielding an estimated final concentration of the complex between 3 and 11  $\mu$ M. The polydisperse  $\alpha$ B-crystallin (*Homo sapiens*, monomer mass 20.2 kDa) used to demonstrate separation of overlapping peaks was a gift from the Laboratory for Biocrystallography at KU Leuven, Belgium, and was used at a concentration of 1.3 mg/mL, also in 100 mM

aqueous ammonium acetate. All experiments were carried out on Synapt G2 and G2-S HDMS mass spectrometers (Waters Corporation, Wilmslow, UK) in TOF mode, unless indicated otherwise. Approximately 5  $\mu$ L of protein solution was transferred to an in-house prepared gold-coated capillary and infused into the mass spectrometer using the nanoflow version of the Z-spray ion source, using a capillary voltage of 1.0–1.3 kV, minimal nanoflow gas pressure, and a backing pressure of 5 mbar. The implementation of ETD on Synapt instruments has been described in detail elsewhere [30] and tuning of the glow discharge was as described earlier [24]. The time windows during which protein cations and ETD reagent anions were accumulated in the trap cell were 1.0 s and 0.1 s, respectively. Traditionally, specific proton transfer reagents such as perfluoro-1,3-dimethylcyclohexane (PDCH) are used for charge-reduction studies [15]. However, standard ETD reagents were used for these experiments: 1,4-dicyanobenzene on the Synapt G2 (fitted with a 32 k quadrupole), and p-nitrotoluene on the Synapt G2-S (8 k quadrupole). Use of either reagent led to similar spectra and showed more efficient charge reduction than PDCH (data not shown).

Instrument settings were as follows on both Synapt platforms: trap pressure 8e-2 mbar, trap collision energy 10 V, trap DC bias 11 V (45 V in Mobility mode), transfer pressure 6e-3 mbar (2e-2 mbar in Mobility mode), transfer collision energy 5 V, detector voltage 3000 V, sampling cone 60–120 V, trap wave height 0.5–0.7 V (1.6–1.9 V in Mobility mode) (sampling cone voltage and trap wave height optimized for each protein complex). For the ion mobility experiments, the IM wave height was 30 V, IM wave velocity 1000 m/s, and the pressure in the IM cell was 4.3 mbar (He gas flow 180 mL/min; IM cell gas flow 50 mL/min).

## Results and Discussion

The mass spectra displayed on the left in Figure 1 show the charge state distributions of native hemoglobin, concanavalin a, alcohol dehydrogenase, pyruvate kinase, and L-glutamic dehydrogenase, acquired in positive ion mode without the introduction of ETD reagent anions into the instrument (glow discharge emitter switched off). The spectra shown in Figure 1a were acquired on a Synapt G2 (up to 100,000  $m/z$ ), and those in Figure 1b on a Synapt G2-S instrument (up to 120,000  $m/z$ ). The charge state that was selected in the quadrupole for charge reduction is indicated in red. The result of ETD conditions, which promote extensive charge reduction of the complexes, is shown on the right-hand side of Figure 1. Interestingly, a bi- or trimodal charge state distribution is typically observed, with a first intensity maximum in close proximity to the selected precursor ions, whereas the others are located at much lower charge states. The gradual decrease in signal intensity above 50,000  $m/z$  is most likely due to less efficient ion transmission and reduced sensitivity of the detector in the high  $m/z$  range. Another striking feature of the spectra in Figure 1 is the peak broadening observed with increasing  $m/z$ . It should be noted,

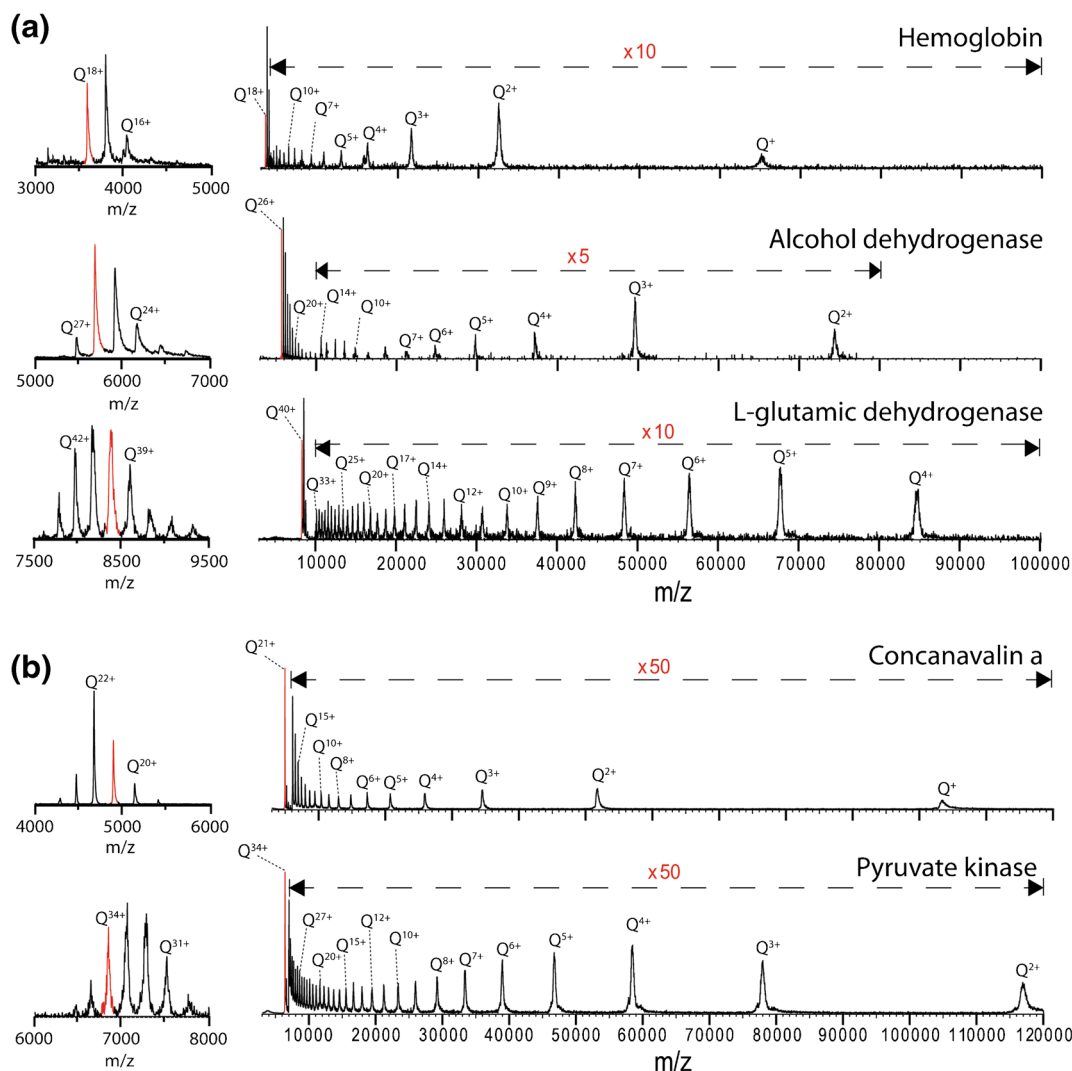


**Figure 1.** Left column: native charge state distributions of hemoglobin, alcohol dehydrogenase, L-glutamic dehydrogenase, concanavalin a, and pyruvate kinase with the precursor charge state in red. Right column: product ion spectra with charge-reduced complex signals. The spectra in (a) were acquired on the Synapt G2 in the mass range 3000–100,000  $m/z$ , whereas the spectra in (b) were acquired on the G2-S, from 3000–120,000  $m/z$

however, that the actual resolution of the peaks, defined as  $(m/z)/(\Delta m/z)$ , either remains constant (e.g., in the case of L-glutamate dehydrogenase) or decreases by a factor of less than two (e.g., for hemoglobin). Another possible reason for apparent peak broadening is the formation of adducts with the ETD reagent [37, 38]. As the mass of the anion (128 Da for the 1,4-dicyanobenzene used in this study) is between 0.04% and 0.2% of the mass of the complexes studied here, the resulting adduct peaks would not be resolved in the spectra shown in Figure 1. The observed peak widths are, however, only compatible with a few adducts.

Whereas the charge-reduced tetramers are annotated as  $Q^{n+}$  for the sake of simplicity, it should be noted that these are not the same  $[Q+nH]^{n+}$  charge states produced by electrospray ionization, but rather the products of a combination of proton transfer and nondissociative electron transfer (ETnoD), which are both known to occur under these conditions [24, 37–40]. It

would, therefore, be more accurate to consider them as  $[Q+xH]^{n+}$ , with  $n \leq x \leq N$ , where  $N$  is the charge state of the precursor. Whilst we are still investigating the precise mechanism of this extensive charge reduction up to very high  $m/z$ , it was proven to be necessary to increase the acceleration voltages after the ETD reaction cell (trap cell) in order to promote the effect. Both the “trap DC bias” (potential difference between the trap cell exit and the traveling wave ion mobility (TWIMS) cell entry), and the “transfer collision energy” setting (ion acceleration into the argon pressurised region of the transfer cell) are effective in this regard. Increased ion acceleration through both voltage offsets enables the detection of crETD products at very high  $m/z$ , leading to similar spectra as demonstrated in TOF mode for alcohol dehydrogenase (Figure 2). The maximum of the lower charge state distribution shifts to the right when increased collisional activation energy (post-ETD

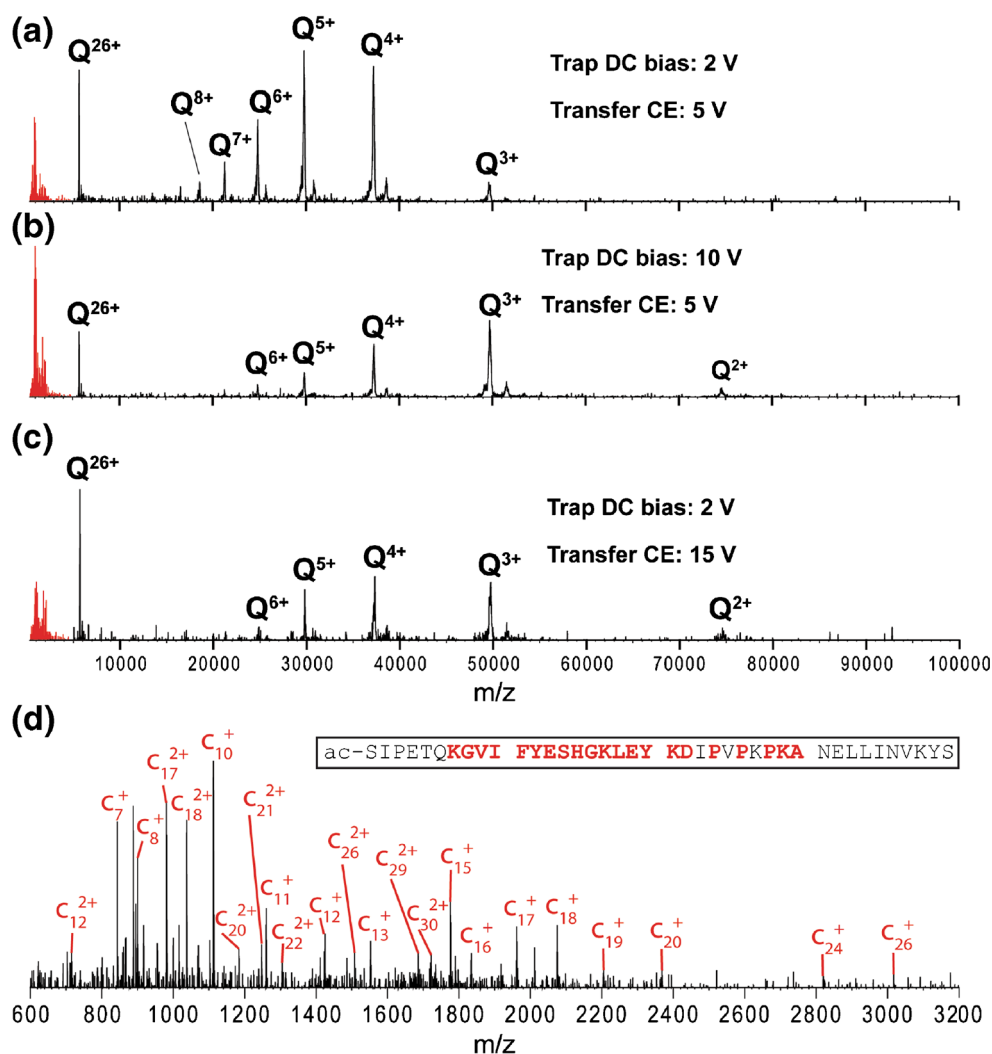


**Figure 2.** (a-c) Alcohol dehydrogenase spectra showing the effect of post-ETD ion acceleration. N-terminal ETD fragments (predominantly singly and doubly charged) are indicated in red at low  $m/z$ . Panel (d) zooms in on the fragments present in panel (b), from 600 to 3200  $m/z$  and some of the peaks are annotated to illustrate the low fragment charge states. The inset shows the observed sequence coverage in the first 40 residues of the monomer

acceleration) is applied as shown in Figure 2b (increased trap DC bias) and Figure 2c (increased transfer CE).

Increasing the voltage offsets in the various stages of the instrument is known to provide improved transmission for high  $m/z$  ions [41, 42], but as the ETD products undergo energetic collisions with the bath gas (which converts ion kinetic energy into internal energy), they will also experience supplemental collisional activation. This could lead to some form of charge-stripping. In order to investigate whether the charge-reduction already occurs in the trap cell, concomitant with ETD, or rather later in the instrument as suggested by the effect of post-ETD acceleration voltages, we also performed charge reduction of alcohol dehydrogenase (ADH) in ion mobility mode (see Figure 3). Under the conditions used here, which favor good ion mobility resolution but should leave the ETD processes in the trap cell unaffected, high  $m/z$  ion transmission was limited and we only observed crETD products up to the 15+ ion. From the uncalibrated data (Figure 3a), it already becomes apparent

that each charge state appears at a different arrival time, while they would share the same drift time if charge reduction had occurred post-ion mobility separation (e.g., in the transfer cell). This leaves the possibility that charge reduction happens before, or during, ion mobility separation. In the latter case, if the exact time point of the charge reduction event during T-wave separation was not defined, ions would switch their charge state somewhere along the mobility cell. Consequently, they would spend variable amounts of time as precursor and charge-reduced species, respectively (somewhat analogous to metastable ions in TOF post-source decay) and we should see a significant broadening of the ion mobility signal for these crETD products (vertical “smearing” in Figure 3a). We observe, however, that the width of the drift time profiles remains largely the same for the observed charge states. Further to this, we also calculated the collision cross-section of these individual charge states (see Table 1) and found that they are essentially the same, apart from the well-known Coulombic effect of



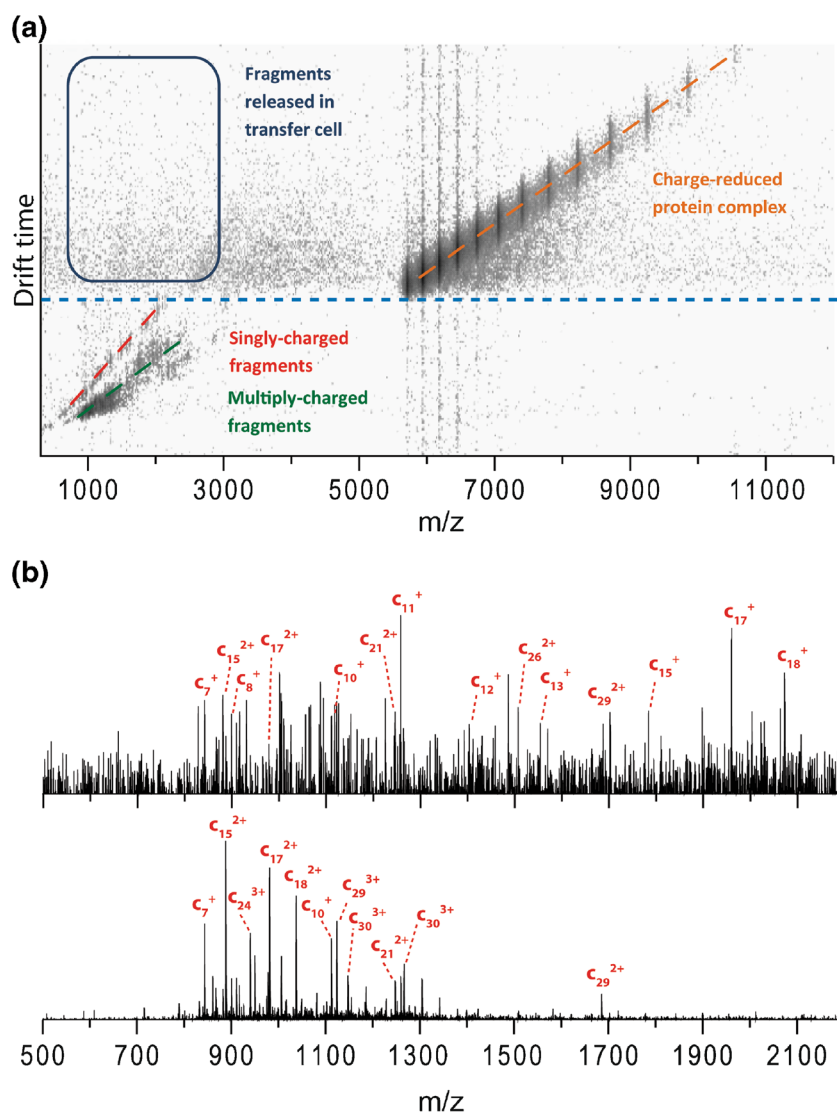


**Figure 3.** (a) Result of charge reduction of 26+ ADH in Mobility mode, represented as a 2D-plot. Fragments released before and after IM separation are easily distinguished based on drift time (below and above the horizontal dashed line, respectively), and singly charged fragments released before IM are separated from multiply charged ones. The fragment spectra in panel (b) were generated by extracting the full  $m/z$  range at drift times above (top) and below (bottom) the horizontal dashed line in panel (a). The highest  $m/z$  fragment observed in the bottom spectrum is  $c_{29}^{2+}$ , at 1685  $m/z$ , and singly charged fragments in this spectrum only span the range between  $c_7^+$  and  $c_{12}^+$ . In the top spectrum, singly charged fragments are observed from  $c_7^+$  to  $c_{18}^+$ , spanning the range up to 2074  $m/z$ .

increasing charge on protein complexes, which makes them appear increasingly larger in the same way as native charge states would, and similar to results reported by Campuzano and Schnier [35]. Taken together, we regard this as evidence that the processes that reduce the charge state as far the 15+ ion must have happened prior to ion mobility separation (i.e., in the trap cell and/or the helium-filled entry stage to the ion mobility cell). While this would suggest that the observed effect of increased post-ETD acceleration voltages, which seem to promote the crETD reaction, is due to the improved high  $m/z$  transmission, no such conclusions can be made at this stage for the extensively charge-reduced species. In the absence of ion mobility data for these very high  $m/z$  species, it is still a possibility that subsequent reactions of ETD products such as

e.g., charge stripping can occur in the later stages of the instrument (beyond the trap cell).

We also investigated the effect of the trap wave height on the crETD reaction, with all other settings kept constant (see Supplementary Information S-1). The trap wave height is known to determine the extent of interaction between cations and reagent anions (somewhat similar to an “ETD reaction time” in 3D traps) [43]. We observe that the abundance of crETD ions relative to the intact precursor ions increases when the trap wave height is lowered from 2 to 0.6 V. At even lower wave heights, only two charge distributions remain, the first adjacent to the precursor charge state and the second at very high  $m/z$ . These data show that different, competing processes are causing precursor charge reduction in ETD, leading to quite

**Table 1.** Calculated Collision Cross-Sections (CCS) for the Charge states of ADH Observed in Figure 3

<i>z</i>	<i>m/z</i>	CCS (Å <sup>2</sup> )
26	5678	7501
25	5906	7427
24	6154	7480
23	6422	7402
22	6715	7387
21	7036	7336
20	7389	7365
19	7777	7275
18	8212	7182
17	8698	7137
16	9234	7075
15	9868	7017

The charge states of ADH generated by native ESI (23+ to 26+) were used to calibrate the spectrum and CCS values were calculated using a logarithmic fit as described by Ruotolo and colleagues [49, 50]

complicated dependencies of the observed charge state distributions on ETD reaction control parameters. We are currently investigating this phenomenon further, in particular processes that lead to the generation of the very high *m/z* ions.

In order to demonstrate the use of the crETD method for the separation of overlapping peaks, we selected the protein complex  $\alpha$ B-crystallin since it is known to be polydisperse [44–46]. This protein forms large oligomers with variable stoichiometry in solution. Figure 4a shows the native spectrum, displaying significant peak overlap. Peaks from the 16- to 18-mer are relatively well resolved in the 7500–8500 *m/z* region (calculated *m/z* values indicated with dashed lines; charge states approximately 41+ to 46+), but these species alone cannot account for the broad distribution of peaks observed, which also contains larger oligomers. For example, the peak with a maximum around 8500 *m/z* cannot be explained by only these two species, but likely also has a contribution from the 20-mer. Benesch and colleagues have reported that these oligomers somewhat favor a 2*n* stoichiometry [47, 48], but even with this prior knowledge, assignment of the region between 8500 and 10,000 *m/z* is not possible because of peak overlap. In order to overcome this problem, they used CID [45, 47, 48] to eject highly-charged monomers (sometimes in multiple steps) in order to achieve better separation between the resulting charge-reduced (*n*-1)- and (*n*-2)-mers. We selected the poorly resolved 8500–10,000 *m/z* region in the quadrupole by setting the MS/MS mass to 9000, with LM and HM resolutions both set to 2. ETD-driven charge reduction of this complex signal generated the spectrum shown in Figure 4b, which shows much more separation between adjacent peaks, which we could assign mainly to the 20-, 22-, and 24-mer, with smaller contributions from the 18- and 23-mer. A zoomed-in view of the region with the most spacing between adjacent peaks is shown in Figure 4c, along with calculated *m/z* values for the different oligomers (dashed lines; charge states 7+ to 12+). Only a few signals here are still subject to possible superposition of different

oligomer charge states, mainly the peak around 40,500 *m/z*, which can theoretically have contributions from any oligomer with an even number of subunits. Two limitations of this approach at this stage are the peak broadening discussed earlier, and the difficulty with calibrating such an extremely large *m/z* range accurately. The case of polydisperse  $\alpha$ B-crystallin nevertheless demonstrates that even a relatively complex mix of overlapping signals can be somewhat deconvoluted by charge-reduction MS.

Previous charge reduction experiments carried out in ion traps, using high proton affinity anionic reagents such as PDCH [15], reported no evidence of dissociation. The work carried out here, however, using conventional ETD reagents with supplemental activation, not only showed significant charge reduction but also provided sequence-specific ETD fragment ions at the same time. These are visible for alcohol dehydrogenase in Figures 2 and 3, where, to the left of the precursor, N-terminal ETD fragments from *c*<sub>7</sub> to *c*<sub>30</sub> are observed, resulting from the cleavage of surface-exposed residues as previously reported [24]. In this earlier work, fragments smaller than *c*<sub>13</sub> appeared as singly charged ions, fragments *c*<sub>14</sub> to *c*<sub>22</sub> only appeared doubly charged, and fragments *c*<sub>24</sub> to *c*<sub>30</sub> appeared exclusively triply charged, with the exception of *c*<sub>26</sub>, where the 2+ and 3+ fragment ions coexist. Interestingly, under conditions optimized for charge reduction, these fragments now also appear at lower charge states, typically at 1+ or 2+, as illustrated in Figure 2d. Virtually no CID fragmentation was observed. Since the tuning parameters, particularly the supplemental activation, differ from the optimal settings for native ETD fragmentation, sequence coverage was lower than reported previously [24], where only limited charge reduction of 26+ alcohol dehydrogenase (down to the 20+ charge state) was observed. Similar behavior is observed for hemoglobin, as illustrated in Supplementary Figure S-2. Two mechanisms could lead to the observation of these low-charged fragments: Fragments could be released and the charge state subsequently reduced, or it could be that the charge-reduced precursors—specifically ETnoD products—are releasing fragments upon supplemental activation [24–27]. We can distinguish these two possibilities using ion mobility (see Figure 3), where fragments released in the trap cell appear at lower drift times than those released after supplemental activation (which share the drift time of the charge-reduced precursor). In this way, we can distinguish both types of fragments by dividing the spectrum into high- and low-drift time sub-spectra. Signal intensity in the former spectrum in the 500–2000 *m/z* range is fairly low, but singly charged fragments spanning the range from *c*<sub>7</sub>–*c*<sub>18</sub> are observed. In the low-drift time spectrum, however, singly charged fragments are only observed up to *c*<sub>12</sub><sup>+</sup>, suggesting that charge reduction predominantly occurs before fragmentation. The relatively low intensity of the singly charged fragments and the fact that singly charged fragments do not appear up to *c*<sub>26</sub><sup>+</sup> (compare with Figure 2d) can be explained by the reduced transmission of very high *m/z* species in IM mode.

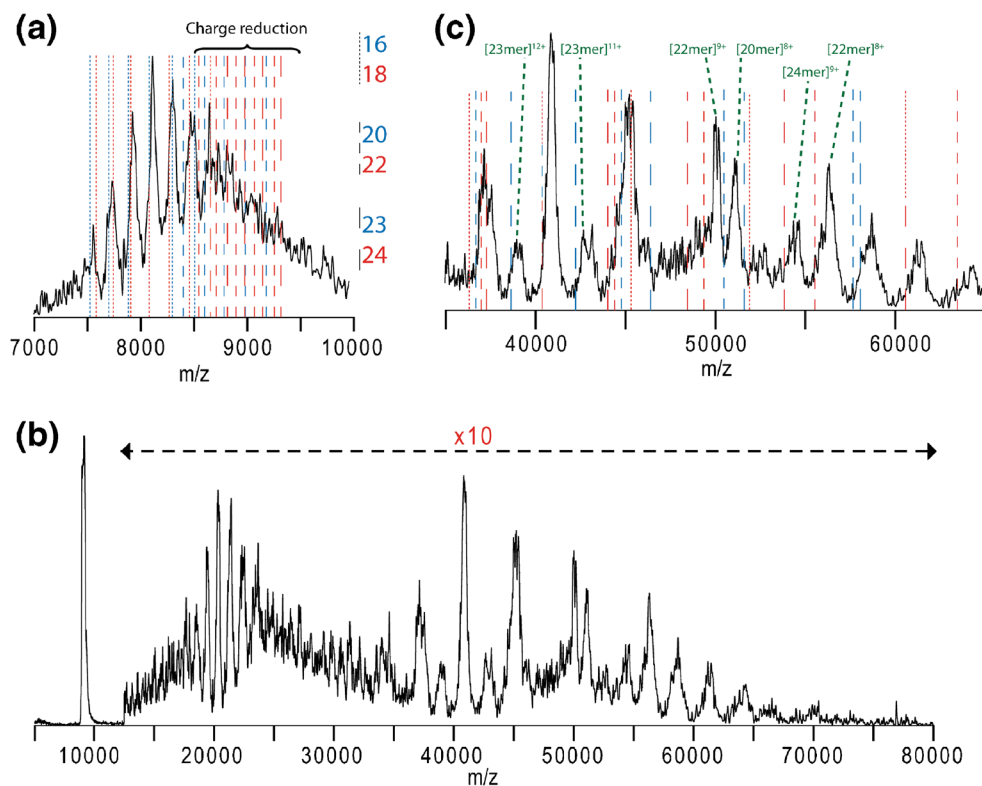


**Figure 4.** Charge reduction of polydisperse  $\alpha$ B-crystallin. Panel (a) shows the native mass spectrum, characterized by significant peak overlap. Although the peaks between 7500 and 8500  $m/z$  appear fairly well resolved, overlap makes it difficult to distinguish the 16- and 18-mer (calculated  $m/z$  values indicated by dashed lines), complicating the assignment. The signals between 8500 and 10,000  $m/z$  correspond to larger oligomers, but are not sufficiently resolved to assign them, even if only those oligomers consisting of an even number of subunits are considered. The spectrum in panel (b) was acquired by isolating the ions in the poorly resolved region in the quadrupole and subjecting them to charge reduction, allowing confident assignment. Panel (c) zooms in on the 35,000–65,000  $m/z$  region of panel (b), with the theoretical  $m/z$  values of the oligomers indicated by dashed lines and a few of the major species labeled

## Conclusions

This work reports for the first time charge-reduced product ions for native noncovalent protein complexes up to and beyond  $m/z$  100,000 on an unmodified QTOF operating in ETD mode. Concomitant with the charge reduction (crETD), top-down fragments from the protein complexes are also observed. These sequence-specific ions originate from the surface-exposed N-terminal regions of the subunits and are detected at low charge states, which simplify their assignment.

The crETD approach promises to be very useful for the manipulation of charge states of protein ions in the gas phase, rather than in solution or during the electrospray process, without the need for modifications to the instrument. In combination with ion mobility, it allows to better understand the relationship between electrospray-generated and gas phase charge states, and the effect of charge state on the global conformation (collision cross section) of proteins and complexes.

Extensive charge reduction of noncovalent complexes generated by native ESI by up to nearly 40 charges was achieved for ions with masses of several hundred kDa.

Using this approach, the very heterogeneous signal generated by a native, polydisperse protein complex was partially deconvoluted, simplifying the identification of the major species present in the spectrum. Future work will take advantage of the ability to charge-reduce native biomolecular assemblies post-electrospray, paving the path to extensive studies of protein gas-phase conformations in response to electrostatic effects.

## Acknowledgments

The authors thank the Research Foundation - Flanders (FWO) for funding a Ph.D. fellowship (F.L.). F.S. is a Francqui Research Professor at UA. The Synapt G2 mass spectrometer is funded by a grant from the Hercules Foundation - Flanders. Financial support from the Flemish Institute for Technological Research (VITO) is gratefully acknowledged. The authors' thanks also go to Michelle Heirbaut, Stephen Weeks, and Sergei Strelkov (Laboratory for Biocrystallography at KU Leuven) for providing the  $\alpha$ B-crystallin sample. Finally, the authors thank the reviewers for their valuable comments.

## References

1. Benesch, J.L., Ruotolo, B.T., Sobott, F., Wildgoose, J., Gilbert, A., Bateman, R., Robinson, C.V.: Quadrupole-time-of-flight mass spectrometer modified for higher-energy dissociation reduces protein assemblies to peptide fragments. *Anal. Chem.* **81**, 1270–1274 (2009)
2. Konijnenberg, A., Butterer, A., Sobott, F.: Native ion mobility-mass spectrometry and related methods in structural biology. *Biochim. Biophys. Acta* **1834**, 1239–1256 (2013)
3. Hall, Z., Robinson, C.V.: Do charge state signatures guarantee protein conformations? *J. Am. Soc. Mass Spectrom.* **23**, 1161–1168 (2012)
4. Benesch, J.L.P., Ruotolo, B.T., Simmons, D.A., Robinson, C.V.: Protein complexes in the gas phase: Technology for structural genomics and proteomics. *Chem. Rev.* **107**, 3544–3567 (2007)
5. Erba, E.B.: Investigating macromolecular complexes using top-down mass spectrometry. *Proteomics* **14**, 1259–1270 (2014)
6. Horn, D.M., Zubarev, R.A., McLafferty, F.W.: Automated reduction and interpretation of high resolution electrospray mass spectra of large molecules. *J. Am. Soc. Mass Spectrom.* **11**, 320–332 (2000)
7. Kaur, P., O Connor, P.B.: Algorithms for automatic interpretation of high resolution mass spectra. *J. Am. Soc. Mass Spectrom.* **17**, 459–468 (2006)
8. Tseng, Y.H., Uetrecht, C., Heck, A.J., Peng, W.P.: Interpreting the charge state assignment in electrospray mass spectra of bioparticles. *Anal. Chem.* **83**, 1960–1968 (2011)
9. Morgner, N., Robinson, C.V.: Massign: an assignment strategy for maximizing information from the mass spectra of heterogeneous protein assemblies. *Anal. Chem.* **84**, 2939–2948 (2012)
10. Tseng, Y.H., Uetrecht, C., Yang, S.C., Barendregt, A., Heck, A.J.R., Peng, W.P.: Game-theory-based search engine to automate the mass assignment in complex native electrospray mass spectra. *Anal. Chem.* **85**, 11275–11283 (2013)
11. Sivalingam, G.N., Yan, J., Sahota, H., Thalassinou, K.: Amphitrite: a program for processing travelling wave ion mobility mass spectrometry data. *Int. J. Mass Spectrom.* **345**, 54–62 (2013)
12. Stengel, F., Baldwin, A.J., Bush, M.F., Hilton, G.R., Lioe, H., Basha, E., Jaya, N., Vierling, E., Benesch, J.L.: Dissecting heterogeneous molecular chaperone complexes using a mass spectrum deconvolution approach. *Chem. Biol.* **19**, 599–607 (2012)
13. Scaif, M., Westphall, M.S., Krause, J., Kaufman, S.L., Smith, L.M.: Controlling charge states of large ions. *Science* **283**, 194–197 (1999)
14. Scaif, M., Westphall, M.S., Smith, L.M.: Charge reduction electrospray mass spectrometry. *Anal. Chem.* **72**, 52–60 (2000)
15. Reid, G.E., Wells, J.M., Badman, E.R., McLuckey, S.A.: Performance of a quadrupole ion trap mass spectrometer adapted for ion/ion reaction studies. *Int. J. Mass Spectrom.* **222**, 243–258 (2003)
16. Prentice, B.M., McLuckey, S.A.: Gas-phase ion/ion reactions of peptides and proteins: acid/base, redox, and covalent chemistries. *Chem. Commun.* **49**, 947–965 (2013)
17. Robb, D.B., Brown, J.M., Morris, M., Blades, M.W.: Method of atmospheric pressure charge stripping for electrospray ionization mass spectrometry and its application for the analysis of large poly(ethylene glycol)s. *Anal. Chem.* **86**, 9644–9652 (2014)
18. Kaiser, R.E., Cooks, R.G., Stafford, G.C., Syka, J.E.P., Hemberger, P.H.: Operation of a quadrupole ion trap mass spectrometer to achieve high mass/charge ratios. *Int. J. Mass Spectrom. Ion Processes* **106**, 79–115 (1991)
19. Geels, R.B., van der Vies, S.M., Heck, A.J., Heeren, R.M.: Electron capture dissociation as structural probe for noncovalent gas-phase protein assemblies. *Anal. Chem.* **78**, 7191–7196 (2006)
20. Xie, Y., Zhang, J., Yin, S., Loo, J.A.: Top-down ESI-ECD-FT-ICR mass spectrometry localizes noncovalent protein-ligand binding sites. *J. Am. Chem. Soc.* **128**, 14432–14433 (2006)
21. Zhang, H., Cui, W., Wen, J., Blankenship, R.E., Gross, M.L.: Native electrospray and electron-capture dissociation in FTICR mass spectrometry provide top-down sequencing of a protein component in an intact protein assembly. *J. Am. Soc. Mass Spectrom.* **21**, 1966–1968 (2010)
22. Zhang, H., Cui, W.D., Wen, J.Z., Blankenship, R.E., Gross, M.L.: Native electrospray and electron-capture dissociation FTICR mass spectrometry for top-down studies of protein assemblies. *Anal. Chem.* **83**, 5598–5606 (2011)
23. Zhang, H., Cui, W.D., Gross, M.L.: Native electrospray ionization and electron-capture dissociation for comparison of protein structure in solution and the gas phase. *Int. J. Mass Spectrom.* **354**, 288–291 (2013)
24. Lermite, F., Konijnenberg, A., Williams, J.P., Brown, J.M., Valkenburg, D., Sobott, F.: ETD allows for native surface mapping of a 150 kDa noncovalent complex on a commercial Q-TWIMS-TOF instrument. *J. Am. Soc. Mass Spectrom.* **25**, 343–350 (2014)
25. Pitteri, S.J., Chrisman, P.A., Hogan, J.M., McLuckey, S.A.: Electron transfer ion/ion reactions in a three-dimensional quadrupole ion trap: reactions of doubly and triply protonated peptides with SO<sub>2</sub><sup>+</sup>. *Anal. Chem.* **77**, 1831–1839 (2005)
26. Swaney, D.L., McAlister, G.C., Wirtala, M., Schwartz, J.C., Syka, J.E., Coon, J.J.: Supplemental activation method for high-efficiency electron-transfer dissociation of doubly protonated peptide precursors. *Anal. Chem.* **79**, 477–485 (2007)
27. Xia, Y., Han, H., McLuckey, S.A.: Activation of intact electron-transfer products of polypeptides and proteins in cation transmission mode ion/ion reactions. *Anal. Chem.* **80**, 1111–1117 (2008)
28. Abzalimov, R.R., Kaltashov, I.A.: Electrospray ionization mass spectrometry of highly heterogeneous protein systems: protein ion charge state assignment via incomplete charge reduction. *Anal. Chem.* **82**, 7523–7526 (2010)
29. Pringle, S.D., Giles, K., Wildgoose, J.L., Williams, J.P., Slade, S.E., Thalassinou, K., Bateman, R.H., Bowers, M.T., Scrivens, J.H.: An investigation of the mobility separation of some peptide and protein ions using a new hybrid quadrupole/travelling wave IMS/oa-ToF instrument. *Int. J. Mass Spectrom.* **261**, 1–12 (2007)
30. Williams, J.P., Brown, J.M., Campuzano, I., Sadler, P.J.: Identifying drug metallation sites on peptides using electron transfer dissociation (ETD), collision induced dissociation (CID), and ion mobility-mass spectrometry (IM-MS). *Chem. Commun.* **46**, 5458–5460 (2010)
31. Rand, K.D., Pringle, S.D., Morris, M., Engen, J.R., Brown, J.M.: ETD in a traveling wave ion guide at tuned Z-spray ion source conditions allows for site-specific hydrogen/deuterium exchange measurements. *J. Am. Soc. Mass Spectrom.* **22**, 1784–1793 (2011)
32. Syka, J.E., Coon, J.J., Schroeder, M.J., Shabanowitz, J., Hunt, D.F.: Peptide and protein sequence analysis by electron transfer dissociation mass spectrometry. *Proc. Natl. Acad. Sci. USA* **101**, 9528–9533 (2004)
33. Catalina, M.I., van den Heuvel, R.H., van Duijn, E., Heck, A.J.: Decharging of globular proteins and protein complexes in electrospray. *Chemistry* **11**, 960–968 (2005)
34. Bornschein, R.E., Hyung, S.J., Ruotolo, B.T.: Ion mobility-mass spectrometry reveals conformational changes in charge reduced multiprotein complexes. *J. Am. Soc. Mass Spectrom.* **22**, 1690–1698 (2011)
35. Campuzano, I., Schnier, P.: Coupling electrospray corona discharge, charge reduction and ion mobility mass spectrometry: from peptides to large macromolecular protein complexes. *Int. J. Ion Mobility Spectrom.* **16**, 51–60 (2013)
36. Brown, J.M., Morris, M., Gigante, B., Walling, L., Schnier, P.: Selective ion–ion charge reduction of multiply protonated heterogenous ESI ions. Proceedings of the 59th ASMS Conference on Mass Spectrometry and Allied Topics, Denver, Colorado, WP01:1693 (2011)
37. McLuckey, S.A., Stephenson Jr., J.L.: Ion/ion chemistry of high-mass multiply charged ions. *Mass Spectrom. Rev.* **17**, 369–407 (1998)
38. Pitteri, S.J., McLuckey, S.A.: Recent developments in the ion/ion chemistry of high-mass multiply charged ions. *Mass Spectrom. Rev.* **24**, 931–958 (2005)
39. Gunawardena, H.P., He, M., Chrisman, P.A., Pitteri, S.J., Hogan, J.M., Hodges, B.D., McLuckey, S.A.: Electron transfer versus proton transfer in gas-phase ion/ion reactions of polyprotonated peptides. *J. Am. Chem. Soc.* **127**, 12627–12639 (2005)
40. Liu, J., McLuckey, S.A.: Electron transfer dissociation: effects of cation charge state on product partitioning in ion/ion electron transfer to multiply protonated polypeptides. *Int. J. Mass Spectrom.* **330/332**, 174–181 (2012)
41. Chemushevich, I.V., Thomson, B.A.: Collisional cooling of large ions in electrospray mass spectrometry. *Anal. Chem.* **76**, 1754–1760 (2004)
42. Sobott, F., Hernandez, H., McCammon, M.G., Tito, M.A., Robinson, C.V.: A tandem mass spectrometer for improved transmission and analysis of large macromolecular assemblies. *Anal. Chem.* **74**, 1402–1407 (2002)
43. Sobott, F., Watt, S.J., Smith, J., Edelman, M.J., Kramer, H.B., Kessler, B.M.: Comparison of CID- versus ETD-based MS/MS fragmentation for the analysis of protein ubiquitination. *J. Am. Soc. Mass Spectrom.* **20**, 1652–1659 (2009)
44. Haley, D.A., Horwitz, J., Stewart, P.L.: The small heat-shock protein, alphaB-crystallin, has a variable quaternary structure. *J. Mol. Biol.* **277**, 27–35 (1998)
45. Aquilina, J.A., Benesch, J.L., Bateman, O.A., Slingsby, C., Robinson, C.V.: Polydispersity of a mammalian chaperone: mass spectrometry reveals



- the population of oligomers in alphaB-crystallin. *Proc. Natl. Acad. Sci. USA* **100**, 10611–10616 (2003)
46. Hochberg, G.K., Benesch, J.L.: Dynamical structure of alphaB-crystallin. *Prog. Biophys. Mol. Biol.* **115**, 11–20 (2014)
47. Aquilina, J.A., Benesch, J.L., Ding, L.L., Yaron, O., Horwitz, J., Robinson, C.V.: Phosphorylation of alphaB-crystallin alters chaperone function through loss of dimeric substructure. *J. Biol. Chem.* **279**, 28675–28680 (2004)
48. Aquilina, J.A., Benesch, J.L., Ding, L.L., Yaron, O., Horwitz, J., Robinson, C.V.: Subunit exchange of polydisperse proteins: mass spectrometry reveals consequences of alphaA-crystallin truncation. *J. Biol. Chem.* **280**, 14485–14491 (2005)
49. Ruotolo, B.T., Benesch, J.L., Sandercock, A.M., Hyung, S.J., Robinson, C.V.: Ion mobility-mass spectrometry analysis of large protein complexes. *Nat. Protoc.* **3**, 1139–1152 (2008)
50. Bush, M.F., Hall, Z., Giles, K., Hoyes, J., Robinson, C.V., Ruotolo, B.T.: Collision cross sections of proteins and their complexes: a calibration framework and database for gas-phase structural biology. *Anal. Chem.* **82**, 9557–9565 (2010)